

# THE BEAM DYNAMICS STUDIES OF COMBINED MISALIGNMENTS AND RF ERRORS FOR RIA\*

X. Wu<sup>†</sup>, D. Gorelov, T. Grimm, W. Hartung, F. Marti, and R.C. York  
National Superconducting Cyclotron Laboratory, MSU, East Lansing, MI 48824, USA

*Abstract*

The National Superconducting Cyclotron Laboratory (NSCL) design for the Rare Isotope Accelerator (RIA) driver linac [1] uses superconducting quarter-wave, half-wave and 6-cell elliptical cavities with rf frequencies ranging from 80.5 MHz to 805 MHz with two charge-stripping chicanes. The driver linac requirements include acceleration of light and heavy ions to final beam energies of  $\geq 400$  MeV/nucleon with final beam powers of 100 to 400 kW. The impact of simultaneous misalignment and rf errors for the full RIA driver linac, including the charge-stripping chicanes, on the 6-dimensional beam emittance was evaluated by simulation. Beam loss and large-amplitude beam behaviors were also studied.

## INTRODUCTION

Misalignment and rf errors were previously evaluated for the Rare Isotope Accelerator (RIA) driver linac [2,3]. The NSCL design for this linac [4] is considered in the present study using the computer codes DIMAD [5] and LANA [6,7]. The misalignment and rf error tolerances for the RIA driver linac from the previous analysis are given in Tables 1 and 2.

Table 1: Alignment tolerances.

RIA Driver Linac	Cavity Misalignment		Focusing Element Misalignment	
	$\sigma_{x,y}$ (mm)	$\sigma_{zr}$ (mrad)	$\sigma_{x,y}$ (mm)	$\sigma_{zr}$ (mrad)
Part I	1.0	-	0.25	-
Part II	1.0	-	0.50	-
Part III	1.0	-	1.00	5.0

Table 2: RF error tolerances.

RF Errors	Maximum Value
Phase	0.5°
Amplitude	0.5%

These tolerances were based on the separate beam simulations using DIMAD for misalignment with orbit corrections, and using LANA for rf errors. These evaluations found that the beam centroid distortion is limited and stays within  $\pm 5$  mm for the specified misalignment margins using the proposed correction scheme. It also was found that beam loss of  $\leq 10^{-4}$  is achievable with rf errors of  $\Delta\phi \leq 0.5^\circ$  in phase and  $\Delta E_0 \leq 0.5\%$  in amplitude.

\*Work supported by MSU and NSF PHY 0110253.  
<sup>†</sup>xwu@nscl.msu.edu

To study the impact of the combined misalignment and rf errors in the 80.5 MHz-based RIA driver linac [4] a procedure was established to combine DIMAD and LANA simulations. First, the rf defocusing matrices were generated using LANA and imported into DIMAD. With the inclusion of these matrices, DIMAD was used to establish the transverse focusing lattice for the reference charge beam, to implement misalignment errors, and to apply the orbit correction scheme. The misalignment analysis included all SRF cavities and focusing elements assuming a Gaussian distribution ( $\pm 2\sigma$ ). The alignment correction scheme used least square fitting to minimize orbit deviations at the beam position monitors. The focusing lattice, misalignment errors for cavities and focusing elements, and corresponding corrections were then imported into LANA to perform the final 6-dimensional particle tracking, combining the rf jitter with the misalignment errors. Extensive tracking comparisons were performed to ensure the proper data translation between the two codes. LANA and DIMAD models applied for RIA driver linac were found to be in excellent agreement.

## SIMULATIONS WITH MISALIGNMENTS AND RF ERRORS

### *Part I – Low $\beta$ Section*

Part I of the RIA driver linac accelerates two charge states, 28+ and 29+, of uranium beams from the RFQ to the 1<sup>st</sup> stripping chicane. A total of 153 low  $\beta$  superconducting quarter-wave cavities with frequencies of 80.5 MHz and 161 MHz, and 81 superconducting solenoid magnets were positioned in 18 cryomodules. The SRF cavities in Part I all have an aperture of 30 mm. The initial normalized beam emittance was assumed to be  $0.6 \pi$  mm mrad. The errors were applied with the values given in Tables 1 and 2. Figure 1 shows the two-charge state uranium beam envelope resulting from a typical set of errors after orbit correction in the Part I of the linac. Figure 2 shows the corresponding transverse rms beam emittances along this part. Simulations were performed for multiple seeds and the statistical confidence plots for maximum of the multi-charge beam envelopes, as well as horizontal and longitudinal rms emittances, at the end of this part of the linac are shown in Figure 3. The vertical emittance is the same as horizontal within small statistical error. With 90% confidence, the maximum radial beam size will be about 11-12 mm, well within the SRF cavity aperture. The transverse and longitudinal rms beam emittance growths were  $\sim 30\%$  and  $\sim 25\%$ , respectively.

No beam loss was observed for the  $2 \times 10^5$  particles tracked.

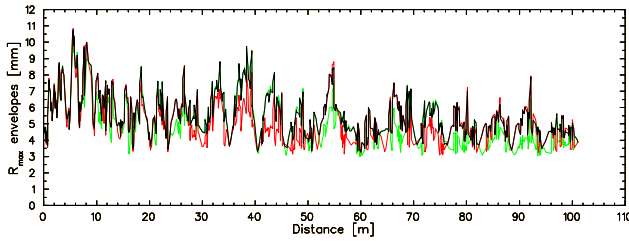


Figure 1: Beam envelopes for multi-charge uranium beam in Part I of the RIA driver linac (red –  $^{238}\text{U}^{29+}$ , green –  $^{238}\text{U}^{28+}$ , black – all charge states) with errors of Tables 1 and 2 after orbit correction.

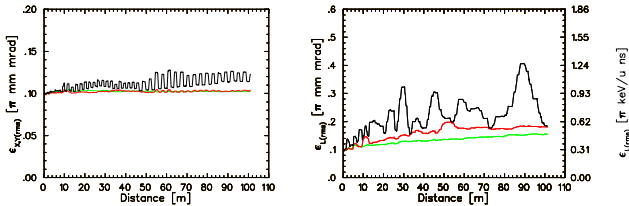


Figure 2: Horizontal (left) and longitudinal (right) rms emittances for  $^{238}\text{U}$  beam in Part I of the linac (red –  $^{238}\text{U}^{29+}$ , green –  $^{238}\text{U}^{28+}$ , black – all charge states) with errors of Tables 1 and 2 after orbit correction.

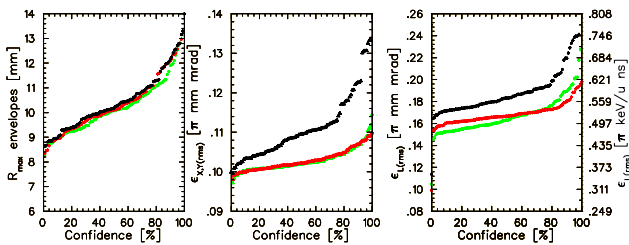


Figure 3: Maximum beam envelopes in Part I of the linac (left), horizontal (middle) and longitudinal (right) rms emittances at the end of Part I vs. statistical confidence (red –  $^{238}\text{U}^{29+}$ , green –  $^{238}\text{U}^{28+}$ , black – all charge states) with errors of Table 1 and 2 after orbit correction.

Simulations were done for misalignment only and for misalignment with rf errors together. Between these two cases, only the longitudinal rms beam emittance growth increased, indicating weak coupling between the transverse and longitudinal motion.

### Part II – Medium $\beta$ Section

Part II of the RIA driver linac will accelerate five charge states,  $73+$  to  $77+$ , of the uranium beam from the 1<sup>st</sup> to the 2<sup>nd</sup> stripping chicane. It consists of 32 cryomodules containing 257 SRF cavities with frequencies of 161 MHz and 322 MHz. A total of 66 superconducting solenoid magnets were used to provide the transverse focusing. The misalignment tolerances,  $\sigma_{x,y}$ , in this section of driver linac are 1.0 mm for all SRF cavities and 0.5 mm for the solenoid magnets. The random rf errors of  $\Delta\phi \leq 0.5^\circ$  in phase and  $\Delta E_0 \leq 0.5\%$  in

amplitude were also included, and a similar multi-seed simulation with LANA performed. The statistical confidence plots for multi-charge beam envelopes, and for transverse and longitudinal rms emittances, are shown in Figure 4. Of 100 seeds, no beam loss was observed in all but 2 pathological cases.

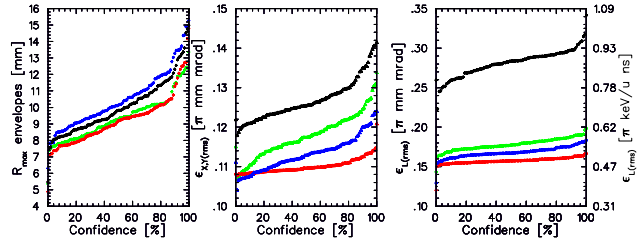


Figure 4: Maximum beam envelopes in Part II of the linac (left), horizontal (middle) and longitudinal (right) rms emittances at the end of Part II with combined misalignment and rf errors vs. statistical confidence (red –  $^{238}\text{U}^{75+}$ , green –  $^{238}\text{U}^{73+}$ , blue –  $^{238}\text{U}^{77+}$ , black – all charge states).

### Part III – High $\beta$ Section

Part III of the RIA driver linac uses 192 6-cell elliptical cavities to accelerate three charge states,  $87+$  to  $89+$ ,  $\text{U}^{238+}$  beams to a final energy of 400 MeV/u. A total of 100 superconducting quadrupole magnets were used to provide the transverse focusing. The misalignment tolerances,  $\sigma_{x,y}$ , in this section of the driver linac are 1.0 mm for all SRF cavities and 1.0 mm for quadrupole magnets. In addition, quadrupole magnets have a skew error (rotation about beam axis) specification of  $\sigma_{zt}$  of 5.0 mrad. The statistical confidence plots for multi-charge beam envelopes, and for transverse and longitudinal rms emittances with combined misalignment and rf errors are shown in Figure 5. No beam loss was observed in any simulated case in this part of the linac.

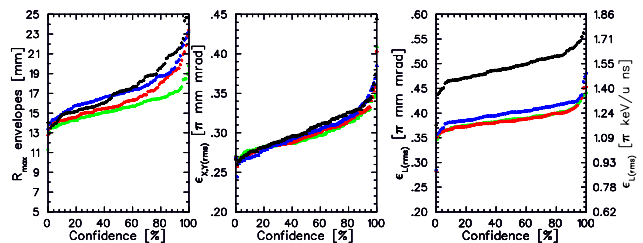


Figure 5: Maximum beam envelopes in Part III of the linac (left), horizontal (middle) and longitudinal (right) rms emittances at the end of Part III with combined misalignment and rf errors vs. statistical confidence (red –  $^{238}\text{U}^{88+}$ , green –  $^{238}\text{U}^{87+}$ , blue –  $^{238}\text{U}^{89+}$ , black – all charge states).

## MISALIGNMENT TOLERANCES FOR CHARGE STRIPPING CHICANES

The two charge-stripping chicane in the RIA driver linac have similar magnetic configurations, each with 8 dipoles, 24 quadrupoles and 16 sextupoles forming a complete 2<sup>nd</sup> order achromat [8]. Chicane #1 has a

stripping energy of 12.7 MeV/u and transports five charge states, 73+ to 77+, of the uranium beam. Chicane #2 strips at 79.0 MeV/u and only transports three charge states, 87+ to 89+. Different position errors,  $\sigma_{x,y}$ , and rotation errors,  $\sigma_{zr}$  for all magnets in chicanes were added together with corrections using correctors in front of each focusing quadrupoles, and multi-charge beam simulations were then performed for both chicanes using DIMAD. The results of the simulations are shown in Figures 6 and 7.

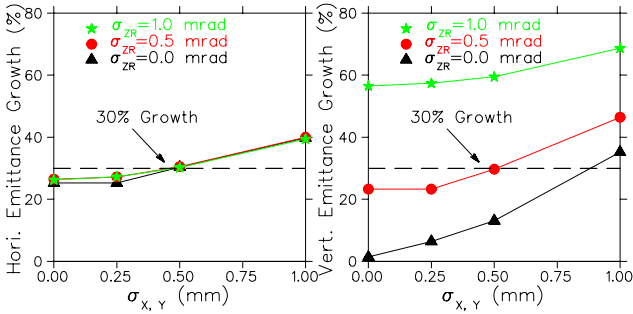


Figure 6: Horizontal (left) and vertical (right) beam emittance growths in charge-stripping chicane #1 due to transverse misalignment errors. Three curves for three different rotational errors ( $\sigma_{zr}$ ) are shown. The dashed line indicates a 30% emittance increase.

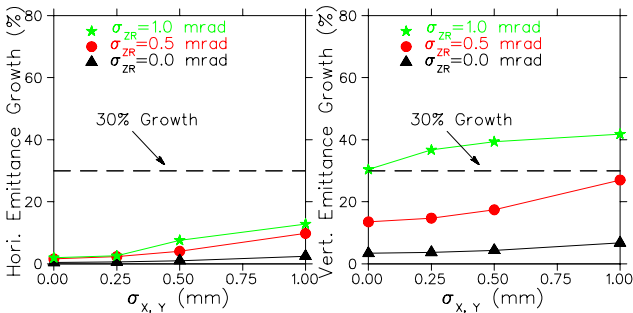


Figure 7: Horizontal (left) and vertical (right) beam emittance growths in charge-stripping chicane #2 due to transverse misalignment errors. Three curves for three different rotational errors ( $\sigma_{zr}$ ) are shown. The horizontal dashed line indicates a 30% emittance increase.

Table 3: Misalignment tolerances for two charge-stripping chicanes in the RIA driver linac

Chicane	Position $\sigma_{x,y}$	Rotation $\sigma_{zr}$
#1	0.5 mm	0.5 mrad
#2	1.0 mm	0.5 mrad

The transverse emittance of both planes increase nearly linearly with the magnet position errors for both stripping chicanes. However, the rotation error ( $\sigma_{zr}$ ) strongly impacts the vertical emittance, while the effect is small in the horizontal plane. This can be understood from the  $x$ - $y$  coupling caused by the rotation error and the large dispersion used to implement the charge state selection. The misalignment tolerances are listed in Table 3, using

as a criterion that the average transverse emittance growth is to be smaller than ~30% in each chicane.

## SUMMARY AND CONCLUSIONS

The impact of combined transverse misalignment and rf errors on the multi-charge beam envelope and transverse, longitudinal emittance growths for different segments of RIA driver linac were investigated by simulation. The results show that the misalignment and rf jitter specifications given are adequate, and that the proposed correction scheme works well for the RIA driver linac. The coupling between the longitudinal and transverse motion in the RIA driver linac is negligible. Although limited transverse and longitudinal emittance growths for multi-charge beam were observed, the impact on the RIA driver linac beam operation should be minimal. Further beam dynamics studies for RIA at NSCL will involve a complete beam simulation from the RFQ through the entire RIA driver linac, with combined rf and misalignment errors, improving LANA’s misalignment correction abilities. Better understanding of the charge-stripping process, and modification of the charge selection chicane design to limit contamination of the superconducting cavities from the stripping process is also needed.

## REFERENCES

- [1] C.W. Leemann, “RIA Facility Project”, Proc. of LINAC 2000, Monterey, CA, 2000.
- [2] X. Wu, D. Gorelov, T. Grimm, W. Hartung, F. Marti, and R.C. York, “The Misalignment and RF Error Analyses for the RIA Driver Linac“ Proc. of LINAC 2002, Gyeongju, Korea, 2002.
- [3] P.N. Ostroumov, “Development of a medium-energy superconducting heavy-ion linac”, Phys. Rev. ST-AB Vol. 5, 030101 (2002).
- [4] D. Gorelov, T. Grimm, W. Hartung, F. Marti, H. Podlech, X. Wu and R.C. York, “Beam Dynamics Studies at NSCL of the RIA Superconducting Driver Linac”, Proc. of EPAC 2002, Paris, France, 2002.
- [5] R. Servranckx, K. Brown, L. Schachinger, and D. Douglas, “User’s Guide to the Program Dimad”, SLAC Report 285, UC-28, May 1985.
- [6] D.V. Gorelov and P.N. Ostroumov, “Application of LANA Code for Design of Ion Linac”, Proc. of EPAC’96, Sitges, June 1996.
- [7] D.V. Gorelov and P.N. Ostroumov, “Simulation of Beam Dynamics Including Space Charge in Proton Linac with Errors”, Proc. of LINAC’98, Chicago, August 1998.
- [8] X. Wu, D. Gorelov, T. Grimm, W. Hartung, F. Marti, H. Podlech, and R.C. York, “The Design of the Isochronous and Achromatic Charge-Stripping Sections for the Rare Isotope Accelerator”, Proc. of EPAC 2002, Paris, France, 2002.